Batteries & Supercaps

Research Article
doi.org/10.1002/batt.202200305

Chemistry Europe
European Chemical Societies Publishing

www.batteries-supercaps.org

"Water-Salt-in-Deep Eutectic Solvent" Method to Optimize Conductivity, Viscosity and Freeze Resistance for Eutectic Electrolytes

Yan Zhang,[a] Yafei Wang,[a] Yangming Zhang,[c] Jingxin Zhao,[d] Yiyang Liu,[e] Ying Guan,*[a] and Yongjun Zhang*[a, b]

A novel and simple "water-salt-in-deep eutectic solvent" (WS-DES) strategy is reported here to increase the ionic conductivity, while reducing the viscosity and freezing temperature of deep eutectic solvent (DES). Upon the addition of water and strong electrolyte salt to the DES of [LiTFSI][EG], the conductivity was increased by 16 times, the viscosity was decreased by 36%, and the freezing temperature was decreased by 30 °C. Additionally, WS-DES strategy can be well applied to electrolytes for supercapacitor devices. Compared to the initial DES, supercapacitors using WS-DES electrolyte have higher specific capacitance, better rate performance, lower IR voltage drop, and lower internal resistance. Moreover, the WS-DES electrolyte also exhibits excellent electrochemical stability under extreme condition even at −40 °C.

Introduction

Future oriented electrochemical energy storage devices require electrolytes with excellent physicochemical properties, especially in terms of conductivity, viscosity, and freezing temperature.[1] Ionic conductivity is the basis of electrolytes, and the level of conductivity seriously affects the electrochemical performance.[1a] On the other hand, viscosity has dramatic impacts on the migration of conducting ions that lower viscosities favor ion migration and higher viscosities discourage electrolyte infusion.[1b] The electrolyte usually will transform into the solid state at temperatures below freezing point and lose its ionic conductivity completely. Therefore, a qualified electrolyte should also have good resistance to freezing.[1c]

Deep eutectic solvents (DES) are very advantageous electrolytes with low cost, simple preparation, environmental friendliness, and wide electrochemical windows, which have gained ever-increasing research progress.[2] However, although DES are generally considered have high ionic conductivity, as with ionic liquids, the conductive mechanism is primarily dominated by the migration of ion pairs between electrodes. Consequently, the ionic conductivity of DES is still weaker than that of electrolytes whose conductivity is carried out in the form of solvated ions. For example, the conductivity of commercial $LiPF_6$ electrolytes can exceed 12 mS cm^{-1} at room temperature,[3] and the conductivity of LiTFSI-H_2O binary electrolytes[4] and aqueous LiCl electrolytes[5] can even reach over 50 mS cm^{-1} and 150 mS cm^{-1} at 20 °C, respectively. Yet the DESs are difficult to achieve this value. In addition, the viscosity of DES is also an issue for practical uses, which also undermines the electrochemical performance as well as the processing complexity.[1b,d,6] Therefore, it is crucial to reduce the viscosity of DES and improve its conductivity and anti-freeze properties for electrolytes in electrochemical energy storage applications.

Herein, a new type of "water-salt-in-DES" (WS-DES) was obtained for the first time by simply adding water and strong electrolyte salts to DES, which substantially improves the conductivity and anti-freeze performance with lower viscosity while maintaining an excellent electrochemical stability (Scheme 1). Firstly, [LiTFSI][ethylene glycol (EG)] was synthesized as the DES. Subsequently, a specific amount of water was added to obtain [LiTFSI][EG]-$x$$H_2O$ (Water-in-DES, W-DES), in which x represents the molar ratio of water to LiTFSI. The addition of water can enhance the conductivity and reduced the viscosity at the same time. Furthermore, the conductivity was boosted by the addition of LiCl. The final solvent is labelled as [LiTFSI][EG]-$x$$H_2O$-$y$LiCl (WS-DES), in which y represents the molar ratio of LiCl to LiTFSI. Meanwhile, the freezing temper-

[a] Dr. Y. Zhang, Dr. Y. Wang, Prof. Y. Guan, Prof. Y. Zhang
Key Laboratory of Functional Polymer Materials and
State Key Laboratory of Medicinal Chemical Biology,
Institute of Polymer Chemistry, College of Chemistry
Nankai University
Tianjin 300071, P. R. China
E-mail: yingguan@nankai.edu.cn
yongjunzhang@nankai.edu.cn
[b] Prof. Y. Zhang
School of Chemistry
Tiangong University
Tianjin 300071, P. R. China
[c] Y. Zhang
State Key Laboratory and Institute of Elemento-organic Chemistry,
College of Chemistry
Nankai University
Tianjin 300071, P. R. China
[d] Dr. J. Zhao
Nanotechnology Center, Institute of Textiles and Clothing,
The Hong Kong Polytechnic University
Hung Hom, Kowloon, Hong Kong 999077, P.R. China
[e] Prof. Y. Liu
School of Chemical Engineering
Zhengzhou University
Zhengzhou 450001, P. R. China

Supporting information for this article is available on the WWW under https://doi.org/10.1002/batt.202200305

Research Article
doi.org/10.1002/batt.202200305
Chemistry Europe
European Chemical Societies Publishing

Scheme 1. Schematic diagram of the "Water-Salt-in-Deep Eutectic Solvent".

ature of DES can also be decreased by adding water or salts. Finally, the obtained WS-DES as electrolytes in supercapacitors were systematically investigated.

Results and Discussion

The molecular structures of LiTFSI and EG are shown in Figure 1(a). Figure 1(b) shows the differential scanning calorimetry (DSC) curves of the eutectic mixtures with different molar ratios. The binary phase diagram of the test results is plotted in Figure 1(c), where the freezing point is defined by the apices of the heat absorption peaks. The freezing point of the eutectic mixture is significantly lowered compared to the pure substance, which indicates new interactions are forming between LiTFSI and EG. Thus, the eutectic point of the LiTFSI and EG mixture is found to be near a molar ratio of 1 : 3. It suggest that the interaction of [LiTFSI][EG] is probably hydrogen bonding

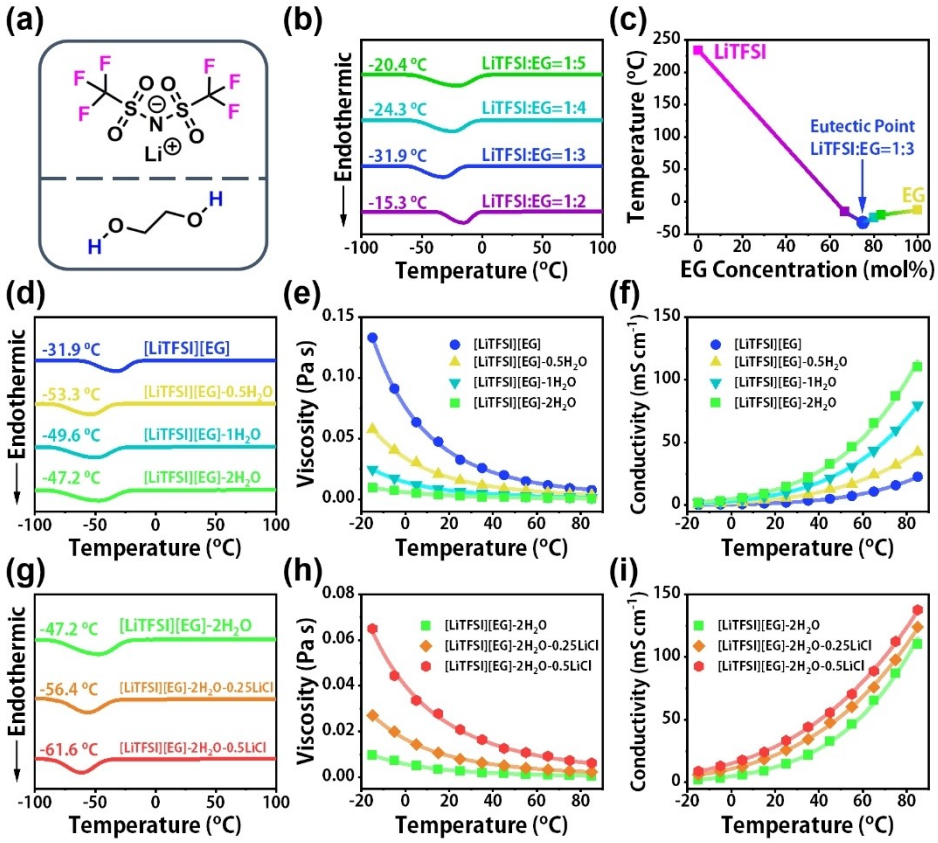

Figure 1. Physicochemical properties. a) Molecular structures of LiTFSI and EG. DSC curves of b) eutectic mixtures, d) W-DES and g) WS-DES. c) The binary phase diagram of [LiTFSI][EG] eutectic mixtures. Variation of viscosity with temperature for e) W-DES and h) WS-DES. Variation of ionic conductivity with temperature for f) W-DES and i) WS-DES.

Research Article
doi.org/10.1002/batt.202200305

between the fluorine atom of LiTFSI and the hydrogen atom from the hydroxyl group of EG. The test results of freezing point, viscosity and conductivity of [LiTFSI][EG] are consistent with previous reports.[7]

Transparent W-DES solvents were obtained by adding different molar ratios of water to [LiTFSI][EG] (Figure S1). The DSC test in Figure 1(d) revealed that the freezing point of [LiTFSI][EG]-xH$_2$O was lowered by 16–21 °C compared to [LiTFSI][EG] without water, which is also consistent with the results of other literature on the addition of water to DES.[8] This can be attributed to the formation of new hydrogen bonding complexes upon the addition of water, the increase in the overall disorder of the solvent (lower entropy difference of the phase transition), and the slow crystallization of the eutectic mixture.[8] In this case, the water molecules are more likely to participate within the DES component to form stronger hydrogen bonds rather than appearing as a separate phase. The addition of water is likely to form a ternary DES, which makes the lowering of the melting point of eutectic electrolyte more significantly. This phenomenon is also similar to the "Water in [ChCl][Urea]",[8c] "water in [ZnCl$_2$][LiTFSI][Urea]"[9] and "water in [LiClO$_4$][Methylsulfonyl-methane]"[10] which reported recently.

Notably, as shown in Figure 1(e), the viscosity of all W-DES decreased significantly after adding water. The higher amount of water added, the more viscosity of the electrolyte decreased. Moreover, as shown in Figure S2 and Table S1, the variation of viscosity (η) with temperature (T) for all solvents is in good accordance with the Arrhenius model [Equation (1)].

$$\eta = Ae^{E_\eta/RT} \tag{1}$$

The introduction of water also substantially improves the conductivity of the solvent (Figure 1f). As shown in Figure S3 and Table S2, the conductivity (κ) versus temperature (T) is also well fitted by the Arrhenius model [Equation (2)].

$$\kappa = \kappa^{o} e^{-E_\kappa/RT} \tag{2}$$

The DSC curves of WS-DES with different LiCl contents are shown in Figure 1(g). The addition of LiCl can further reduce the freezing point of the solvent. The freezing point of [LiTFSI][EG]-2H$_2$O-0.5LiCl is −61.6 °C, which nearly drops 30 °C below that of the [LiTFSI][EG]. The possible reason of the freezing point drop is similar to that the salt lowers the freezing point of water. The ionic electric field in the LiCl salt affects the hydrogen bonding between the solvents and the more diverse components, which cause an increase in the entropy of the new system by making it more difficult to freeze the solvent.[9,11]

Consequently, the addition of LiCl, the viscosity of the solvent increased. The higher amount of salt added, the more viscosity increased (Figure 1h). The variation of viscosity with temperature is also follow the Arrhenius equation (Figure S4 and Table S3). Most impressively, the conductivity of the solvent increased significantly with the increase of LiCl addition (Figure 1i). At 25 °C, the conductivity of [LiTFSI][EG]-2H$_2$O-0.5LiCl is 33.43 mS cm^{-1}, which is 16 times higher than the initial DES (2.14 mS cm^{-1}). The variation of conductivity with temperature also fit the Arrhenius equation [Equation (2)], and the fitting results can be seen in Figure S5 and Table S4. In conclusion, the freezing point, viscosity and ionic conductivity of all solvents tested at 25 °C temperature are summarized in Table S5.

The water state is further determined by ^{17}O NMR spectra (Figure S6). Most of the water is present as free water in the aqueous solution of [LiTFSI][EG], since the ^{17}O resonance of water is detectable at around 0 ppm. The signal shifts to lower frequencies as the [LiTFSI][EG] content increases. This can be mainly attributed to the gradual transition from free water state to bound water state and the resulting change in the space charge distribution of oxygen atoms on water molecules.[1c,9,12] After careful examination, the addition of water only caused a very slight red shift in the characteristic bands of EG and TFSI$^-$, indicating that the eutectic nature of WS-DES remains intact at relatively low water content. For [LiTFSI][EG] with different H$_2$O and LiCl contents, the interactions between the components are clearly shown by obvious changes throughout the Raman spectra in Figure S7. After careful examination, the addition of water only caused a very slight red shift in the characteristic bands of EG and TFSI$^-$, indicating that the eutectic nature of WS-DES remains intact at relatively low water content. Therefore, the definition of W-DES and WS-DES can be reasonably applied to [LiTFSI][EG]-xH$_2$O-yLiCl because the state and chemical environment (i.e., solvent ions, hydrogen bonds) of water in these solvents are significantly changed compared to diluted aqueous solutions of electrolytes.

The Walden classification plot is the classical measure of the ionicity of DES and ionic liquids.[8c,13] The diagram reflects the relationship between the molar conductivity (Λ) and viscosity (η) of the solvents based on Walden's law [Equation (3)].

$$\Lambda\eta = k \tag{3}$$

where k is a constant dependent on temperature and ion size. Figure 2 compares the Walden plot of [LiTFSI][EG], [LiTFSI][EG]-2H$_2$O, [LiTFSI][EG]-2H$_2$O-0.5LiCl at 25 °C. The solid pink line represents the ideal Walden line for the 0.01 M KCl solution in which the ions are completely dissociated and have the same mobility, as well as the mobility of the ions is not determined by the viscosity of the medium.[13b] According to Angell et al,[13b,14] it is superionic if the solvent is above the ideal line. The ionicity of [LiTFSI][EG] is not improved after the addition of water, besides the improvement in conductivity comes mainly from the viscosity decrease. Thus, we believe it is most likely due to the addition of water that raises the free volume in the solvent. Subsequently, the addition of LiCl significantly enhanced the ionicity of the solvents and slightly increased the viscosity. It is worth noting that the lack of free charged species and high viscosities make it difficult to achieve optimal conductivities for DES.[13c] To the best of our knowledge, the [LiTFSI][EG]-2H$_2$O-0.5LiCl has the highest ionicity among DES-based solvents (Figure S8).

Research Article
doi.org/10.1002/batt.202200305
Chemistry Europe
European Chemical Societies Publishing

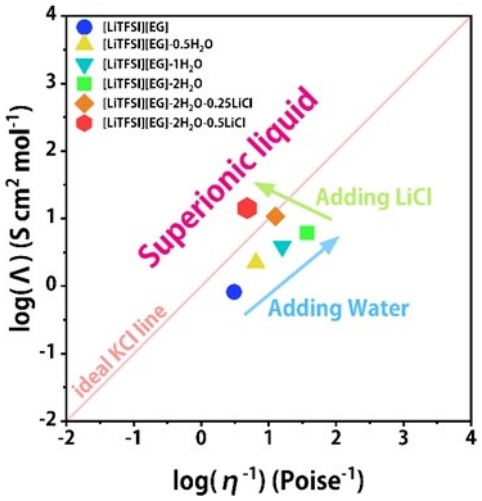

Figure 2. Walden plot at 25 °C for [LiTFSI][EG] and its W-DES, WS-DES.

The thermogravimetric analysis (TGA) results are shown in Figure S9. The addition of LiTFSI to EG to form DES resulted in a substantial increase in thermal stability. Compared to pure DES, the thermal stability became slightly worse at around 150 °C after adding H_2O to [LiTFSI][EG]. After the addition of LiCl, the thermal stability of the obtained [LiTFSI][EG]-$2H_2O$-LiCl became better at high temperature than [LiTFSI][EG] and [LiTFSI][EG]-$2H_2O$. At 400 °C, [LiTFSI][EG]-$2H_2O$-LiCl retained 52.3 % of its initial mass, while [LiTFSI][EG] retained only 45.7 %. This result shows that the addition of trace H_2O and LiCl to DES does not diminish the stability of DES too much. And the addition of LiCl will also improve the stability at high temperatures.

Moreover, the electrochemical performance was systematically investigated. Firstly, the supercapacitor of [LiTFSI][EG] together with its W-DES and WS-DES as electrolyte was tested using symmetric activated carbon electrodes. Figure 3(a) shows the linear sweep voltammetry (LSV) curve for the three solvents. After adding water, the voltage window dropped from 2.51 V to 2.31 V. Further addition of LiCl salt brought the voltage window back up to 2.48 V. The cyclic voltammetry (CV) test was then performed for the [LiTFSI][EG]-$2H_2O$-0.5LiCl electrolyte with the highest conductivity (Figure 3b). In the voltage range of 0–2.2 V, the CV curves show symmetric rectangle shape even with a scan rate at 200 mV s^{-1}, which indicated the highly reversible capacitive performance. The galvanostatic charge-discharge (GCD) curves also exhibits a symmetric triangle shape in Figure 3(c), showing an ideal capacitive behavior.

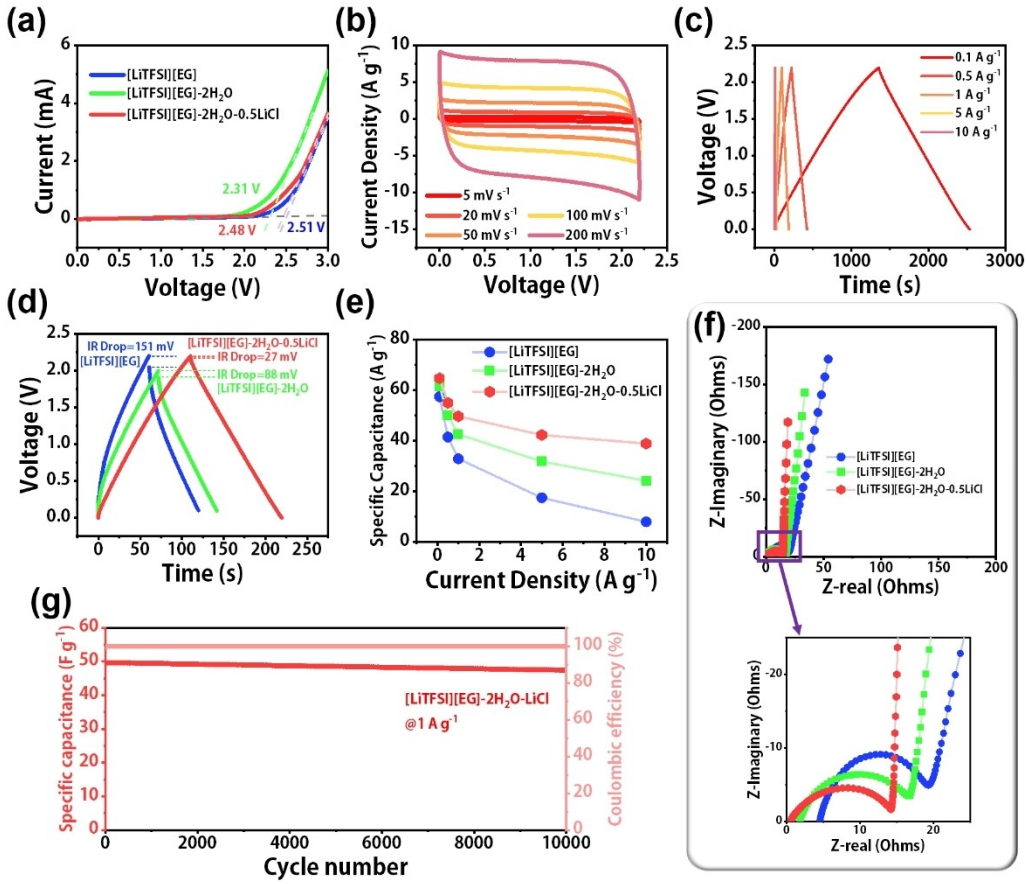

Figure 3. Supercapacitor electrolytes. a) LSV curve of [LiTFSI][EG] and its W-DES and WS-DES. b) CV and c) GCD curves of [LiTFSI][EG]-$2H_2O$-0.5LiCl. d) Comparison of GCD curves at current density of 1.0 A g^{-1}. e) Comparison of gravimetric capacitance. f) Nyquist plot. The below Figure is enlargements of the high-frequency region. g) Cycling performance and Coulombic efficiency of the [LiTFSI][EG]-$2H_2O$-0.5LiCl electrolytes at current density of 1.0 A g^{-1}.

Research Article
doi.org/10.1002/batt.202200305
Chemistry Europe
European Chemical Societies Publishing

Figure 3(d) shows the comparison of the GCD curves of three solvents at the current density of 1.0 A g^{-1}. The specific capacitance is positively correlated with the ionic conductivity of the electrolyte solvents shown in Figure 1(f and i). It is noteworthy that among the eutectic electrolytes currently used in supercapacitors, [LiTFSI][EG]-2H_2O-0.5LiCl is in the leading position in terms of ionic conductivity as shown in Table S6. WS-DES electrolyte has better energy storage performance than W-DES, which is better than DES with worse conductivity. Furthermore, the WS-DES also exhibits the lowest IR drop between the three solvents. The reduction of IR drop is mainly due to the improvement of electrolyte ionic conductivity.[15] The IR drop for [LiTFSI][EG] is 151 mV. After adding water, the [LiTFSI][EG]-2H_2O then decreases to 88 mV. The final IR drop for [LiTFSI][EG]-2H_2O-0.5LiCl after the addition of LiCl salts is 27 mV, which is only 18% of the initial one. Figures 3(e) and S10 show the gravimetric capacitance and Ragone plot respectively. Both results are consistent with the order of the ionic conductivity of the three. The [LiTFSI][EG]-2H_2O-0.5LiCl with the highest conductivity has the best specific capacitance and rate performance.

The three electrolytes were then studied using electrochemical impedance spectroscopy (EIS) (Figure 3f). Nyquist plots suggest that all three electrolytes have ideal electrochemical capacitive behavior, where the imaginary part of the impedance in the low-frequency region is perpendicular to the real part.[16] The internal resistance calculated from the intersection of the plots with the Z-real axis matches perfectly with the conductive sequence of the electrolytes. The internal resistance of [LiTFSI][EG], [LiTFSI][EG]-2H_2O, and [LiTFSI][EG]-2H_2O-0.5LiCl are 4.5 Ω, 1.8 Ω, and 0.6 Ω, respectively. Their internal resistances decline upon the addition of the substance, which is consistent with the IR drop in Figure 3(d). Among them, the [LiTFSI][EG]-2H_2O-0.5LiCl electrolyte has an exceptional cycling stability at room temperature (RT) or 60 °C. Figure 3(g) exhibits the cycling performance at RT, the capacitance decayed only 4.5% after 10000 cycles at the current density of 1.0 A g^{-1}. And the Nyquist curve changes very little at the end of the cycle (Figure S11). Furthermore, the capacitance retention still up to 98.83% after 2000 cycles at 60 °C (Figure S12).

The WS-DES method substantially improves the performance of supercapacitors in different aspects at room temperature. Notably, this method substantially lowers the freezing point of the electrolyte, results in an improvement of the low-temperature performance. The performance of the supercapacitor with [LiTFSI][EG]-2H_2O-0.5LiCl as the electrolyte is greatly improved compared to the initial DES and W-DES at low temperature (Figure S13). Even the temperature drops to −40 °C, the CV curves and GCD curves of the devices still show ideal capacitive energy storage behaviors (Figure 4a and b). At the current density of 0.1 A g^{-1} at −40 °C, the capacitance still has a good performance of 53.0 F g^{-1}, which leads to only 17% decrease compared to room temperature (Figure 4c). Moreover,

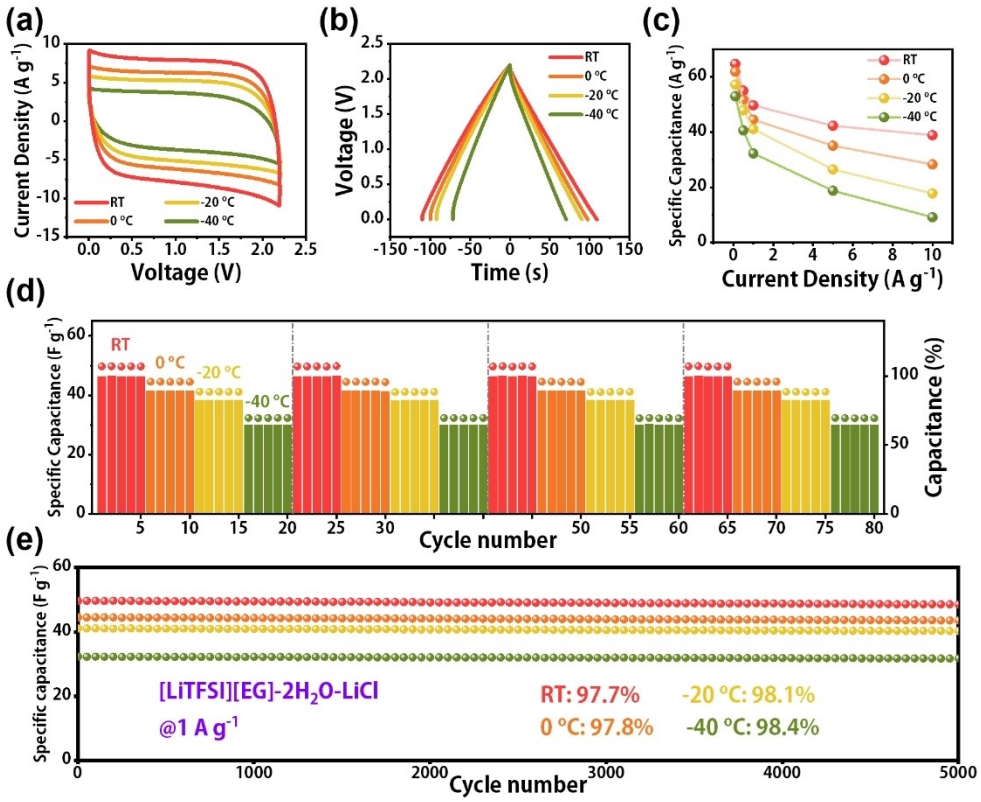

Figure 4. WS-DES electrolytes at various temperatures. a) CV curves at scan rate of 200 mV s^{-1}. b) GCD curves at current density of 1.0 A g^{-1}. c) The comparison of gravimetric capacitance. d) Specific capacitance (dot plot) and capacitance retention (histogram) during cyclic operation at varied temperature ranges. e) Cycling performance of the [LiTFSI][EG]-2H_2O-0.5LiCl electrolytes at current density of 1.0 A g^{-1}.

at a power density of 0.11 kW kg^{-1}, the energy density can still reach 35.63 Wh kg^{-1} at −40 °C (Figure S14).

After cycling tests at four temperature intervals of room temperature, 0 °C, −20 °C, and −40 °C, the capacitances are almost identical to those before cycling (Figure 4d), which demonstrated the good thermal stability of the WS-DES electrolyte and the capacitance stability with temperature fluctuations. The cycling stability of the electrolyte at low temperature was verified at a current density of 1.0 A g^{-1} (Figure 4e). The cycling stability of the device is improving as the temperature decreases. After runs for 5000 cycles at room temperature, 0 °C, −20 °C and −40 °C, the capacitance of the device remained 97.7 %, 97.8 %, 98.1 %, and 98.4 % of the initial capacitance, respectively. And the Nyquist curve changes very little at the end of the cycle even in 40 °C (Figure S15). This result indicates the high stability of WS-DES electrolyte at low temperatures. Moreover, the contrast between low temperature and high cycling performance is most likely due to the suppression of side reactions during ion adsorption-desorption at low temperatures, as reported in other symmetric supercapacitor designs.[17]

Conclusion

In summary, the WS-DES strategy of adding water and LiCl to [LiTFSI][EG] will increase the ionic conductivity while reducing the viscosity and freezing temperature. Compared to initial DES, the ionic conductivity of [LiTFSI][EG]-2H_2O-0.5LiCl after the addition of water and LiCl increased from 2.14 mS cm^{-1} to 33.43 mS cm^{-1}. The viscosity decreased by 36 %, from 32.47 mPa s to 20.84 mPa s. And the freezing temperature decreased by 30 °C (from −31.9 °C to −61.6 °C). The ionicity of the solvents was measured by Walden's law, and it was shown that the "WS-DES" strategy improved the ionicity of DES significantly. Due to the excellent ionic conductivity of [LiTFSI][EG]-2H_2O-0.5LiCl, it can be extremely well used as an electrolyte for supercapacitor from −40 °C to 60 °C. Compared with the initial DES as well as W-DES, the activated carbon supercapacitor using WS-DES electrolyte has higher specific capacitance, better rate performance, lower IR drop, less internal resistance and greater low-temperature performance. This is mainly due to the greatly improved conductivity and freezing temperature. And [LiTFSI][EG]-2H_2O-0.5LiCl electrolyte also has excellent stability at RT and −40 °C, with capacitance retention of 95.5 % after 10000 cycles at RT or 98.4 % after 5000 cycles in −40 °C.

Experimental Section

Materials: Ethylene glycol (EG, 99.9 %, anhydrous grade), LiTFSI (99.9 %, anhydrous grade) and LiCl (99.9 %, anhydrous grade) were purchased from Aladdin. N-methylpyrrolidone (NMP, electronic grade) was purchased from Sigma-Aldrich. Activated carbon (high the specific surface area is about 800 m^2 g^{-1}), LiFePO4, PVDF and Li foil were purchased from HeFei Kejing. Conductive carbon black (Super P) was purchased from Timcal.

Synthesis of "Water-Salt-in-DES": The deep eutectic solvent of [LiTFSI][EG] was synthesized from previous literature.[7] In brief, LiTFSI and EG were mixed in a molar ratio of 1 : 3 and then stirred under nitrogen atmosphere at 80 °C until a clear and transparent liquid was formed. Then a small amount of water was added to it in molar proportion and stirring was continued to obtain [LiTFSI][EG]-$x$$H_2O$ (W-DES), with x representing the molar proportion of water with respect to LiTFSI. Finally, [LiTFSI][EG]-$x$$H_2O$-$y$LiCl (WS-DES) was obtained by adding the corresponding molar amount of LiCl to the solution and stirring until the liquid was clarified, with y representing the molar ratio of LiCl to LiTFSI. All samples were stored in an argon atmosphere glove box before testing. The relative error of water content was measured by Karl-Fischer coulometric titrations method (Table S7).

Physicochemical properties and other characterizations: The freezing temperature of the solvents was obtained by differential scanning calorimetry (DSC) testing using a Netzsch DSC204 thermal analysis system with a cooling rate of 1 °C min^{-1}. The density of the solvents was obtained by measuring the mass of 10.0 mL of solvent using an analytical balance (Sartorius SQP). Viscosity was tested using a TA-500 rheometer. Conductivity measurements were carried out using an LK2000 electrochemical workstation (Lanliko Chemical Electronic High Tech). Data fitting is performed using the orthogonal distance regression. NMR spectra were recorded on a Bruker AV 400 spectrometer at 400 MHz. The TGA was performed on a Rigaku TG-DTA8122 thermogravimetric differential thermal analyser with a heating rate of 10 °C min^{-1}. The Raman spectra were carried out on HORIBA Scientific LabRAM HR Evolution.

Assembly and testing of supercapacitors: The supercapacitor electrode slurry was prepared by mixing and grinding activated carbon, conductive carbon black powder and PVDF binder in an agate mortar in the mass ratio of 8 : 1 : 1, while adding an appropriate amount of NMP solvent. After that, it was coated on the platinum mesh electrode, and two electrodes with the same mass of active materials loading were selected as the positive and negative electrodes of the supercapacitor. The activated carbon loading at the electrode was about 2 mg cm^{-2}. The final symmetrical electrode supercapacitor was assembled from the aforementioned electrodes, glass fibre diaphragm and [LiTFSI][EG]-2H_2O-0.5LiCl electrolyte.

Cyclic voltammetry (CV), galvanostatic charge discharge (GCD) and electrochemical impedance spectroscopy (EIS) were performed using an electrochemical workstation CHI660E (Shanghai Chenhua). The electrochemical stability windows were tested using the linear sweep voltammetry method with a scan rate of 0.5 mV s^{-1}. A battery test system (Land-CT2001 A) was used for the cycle life test of the devices. For test at low temperature, the devices were put into a low temperature storage box (DW-135W118). For test at 60 °C, the devices were put into a constant temperature drying oven. The energy density E and power density P of the DES, W-DES and WS-DES electrolytes at room temperature and low temperature via following formula.

$$E = C\Delta V^2/2$$

$$P = E/\Delta t$$

where C represents the specific capacitance, ΔV represents the voltage window, and Δt represents the discharge time.

Acknowledgements

The authors thank financial support for this work from the National Natural Science Foundation of China (Grants Nos. 52073146, 51625302, 51873091 and 52033004).

Conflict of Interest

The authors declare no conflict of interest.

Data Availability Statement

The data that support the findings of this study are available from the corresponding author upon reasonable request.

Keywords: conductivity · deep eutectic solvent · electrolyte · low temperature · supercapacitor

[1] a) S. Qian, H. Chen, Z. Wu, D. Li, X. Liu, Y. Tang, S. Zhang, *Batteries & Supercaps* **2021**, *4*, 39–59; b) Y. Yamada, J. Wang, S. Ko, E. Watanabe, A. Yamada, *Nat. Energy* **2019**, *4*, 269–280; c) Q. Li, G. Liu, H. Cheng, Q. Sun, J. Zhang, J. Ming, *Chem. Eur. J.* **2021**, *27*, 15842–15865; d) J. Wu, Q. Liang, X. Yu, Q. F. Lü, L. Ma, X. Qin, G. Chen, B. Li, *Adv. Funct. Mater.* **2021**, *31*, 2011102; e) L. Suo, O. Borodin, T. Gao, M. Olguin, J. Ho, X. Fan, C. Luo, C. Wang, K. Xu, *Science* **2015**, *350*, 938–943; f) X. Tian, Q. Zhu, B. Xu, *ChemSusChem* **2021**, *14*, 2501–2515.
[2] a) D. Yu, Z. Xue, T. Mu, *Chem. Soc. Rev.* **2021**, 50, 8596–8638; b) B. B. Hansen, S. Spittle, B. Chen, D. Poe, Y. Zhang, J. M. Klein, A. Horton, L. Adhikari, T. Zelovich, B. W. Doherty, *Chem. Rev.* **2020**, *121*, 1232–1285; c) C.-L. Li, G. Huang, Y. Yu, Q. Xiong, J.-M. Yan, X.-b. Zhang, *J. Am. Chem. Soc.* **2022**, *144*, 5827–5833.
[3] L. O. Valøen, J. N. Reimers, *J. Electrochem. Soc.* **2005**, *152*, A882.
[4] M. S. Ding, K. Xu, *J. Phys. Chem. C* **2018**, *122*, 16624–16629.
[5] A. Yllö, C. Zhang, *Chem. Phys. Lett.* **2019**, *729*, 6–10.
[6] U. Mahanta, S. Choudhury, R. P. Venkatesh, S. SarojiniAmma, S. Ilangovan, T. Banerjee, *ACS Sustainable Chem. Eng.* **2019**, *8*, 372–381.
[7] a) K. T. Tran, L. T. Le, A. L. Phan, P. H. Tran, T. D. Vo, T. T. Truong, N. T. Nguyen, A. Garg, P. M. Le, M. V. Tran, *J. Mol. Liq.* **2020**, *320*, 114495; b) K. T. Tran, T. T. Truong, H. V. Nguyen, Q. D. Nguyen, Q. Phung, P. M. Le, M. V. Tran, *J. Chem.-NY* **2021**, 9940750.
[8] a) S. Liu, Z. Tan, J. Wu, B. Mao, J. Yan, *Electrochem. Sci. Adv.* **2022**, e2100199; b) G. Almustafa, R. Sulaiman, M. Kumar, I. Adeyemi, H. A. Arafat, I. AlNashef, *Chem. Eng. J.* **2020**, *395*, 125173; c) S. Azmi, M. F. Koudahi, E. Frackowiak, *Energy Environ. Sci.* **2022**, *15*, 1156–1171.
[9] J. Zhao, J. Zhang, W. Yang, B. Chen, Z. Zhao, H. Qiu, S. Dong, X. Zhou, G. Cui, L. Chen, *Nano Energy* **2019**, *57*, 625–634.
[10] P. Jiang, L. Chen, H. Shao, S. Huang, Q. Wang, Y. Su, X. Yan, X. Liang, J. Zhang, J. Feng, *ACS Energy Lett.* **2019**, *4*, 1419–1426.
[11] L. Vrbka, P. Jungwirth, *J. Mol. Liq.* **2007**, *134*, 64–70.
[12] M. R. Lukatskaya, J. I. Feldblyum, D. G. Mackanic, F. Lissel, D. L. Michels, Y. Cui, Z. Bao, *Energy Environ. Sci.* **2018**, *11*, 2876–2883.
[13] a) A. Boisset, J. Jacquemin, M. Anouti, *Electrochim. Acta* **2013**, *102*, 120–126; b) U. A. Rana, R. Vijayaraghavan, M. Walther, J. Sun, A. A. Torriero, M. Forsyth, D. R. MacFarlane, *Chem. Commun.* **2011**, *47*, 11612–11614; c) Y. Wang, W. Chen, Q. Zhao, G. Jin, Z. Xue, Y. Wang, T. Mu, *Phys. Chem. Chem. Phys.* **2020**, *22*, 25760–25768.
[14] W. Xu, E. I. Cooper, C. A. Angell, *J. Phys. Chem. B* **2003**, *107*, 6170–6178.
[15] J. Zhao, A. F. Burke, *J. Energy Chem.* **2021**, *59*, 276–291.
[16] P. Taberna, P. Simon, J.-F. Fauvarque, *J. Electrochem. Soc.* **2003**, *150*, A292.
[17] Q. Zheng, X. Li, Q. Yang, C. Li, G. Liu, Y. Wang, P. Sun, H. Tian, C. Wang, X. Chen, *J. Power Sources* **2022**, *524*, 231102.

Manuscript received: July 2, 2022
Revised manuscript received: August 24, 2022
Version of record online: September 22, 2022